ACS Catalysis

RESEARCH ARTICLE

pubs.acs.org/acscatalysis

Mechanism−Performance Relationships of Metal Oxides in Catalyzed HCl Oxidation

Amol P. Amrute,[‡] Cecilia Mondelli,[‡] Miguel A. G. Hevia,[§] and Javier Pérez-Ramírez*[,‡]

[‡]Department of Chemistry and Applied Biosciences, Institute for Chemical and Bioengineering, ETH Zurich, HCI E 125, Wolfgang-Pauli-Strasse 10, CH-8093 Zurich, Switzerland

[§]Institute of Chemical Research of Catalonia (ICIQ), Avenida Países Catalans 16, 43007 Tarragona, Spain

ABSTRACT: The gas-phase oxidation of HCl to Cl_2 over heterogeneous catalysts, known as the Deacon process, is a sustainable way for chlorine recycling in the chemical industry. Mechanistic aspects of this reaction over metal oxides (Cr_2O_3, CeO_2, and MnO_2) have been gathered using the temporal analysis of products (TAP) reactor and compared with the outcome of previous studies over RuO_2 and CuO. The intrinsic features of the TAP technique enable investigation of this demanding reaction in a safe manner and under highly controlled conditions. We have correlated the catalytic activity measured isothermally in a continuous-flow reactor at ambient pressure with mechanistic descriptors derived from the transient responses of reaction products (Cl_2 and H_2O) in the TAP reactor. The order of activity was $RuO_2 > Cr_2O_3 > CeO_2 \sim CuO > MnO_2$. The oxides with lowest activity, MnO_2 and CuO, exhibited bulk chlorination detected by X-ray diffraction and a highly impeded Cl_2 evolution. Chlorination of Cr_2O_3 and CeO_2 during reaction conditions was limited to the surface, as observed with RuO_2. However, catalyst reoxidation over the former two catalysts is more costly. Consequently, RuO_2 possesses the two main features for a suitable Deacon catalyst: limited chlorination, conferring stability; and easier Cl_2 evolution, allowing low-temperature operation.

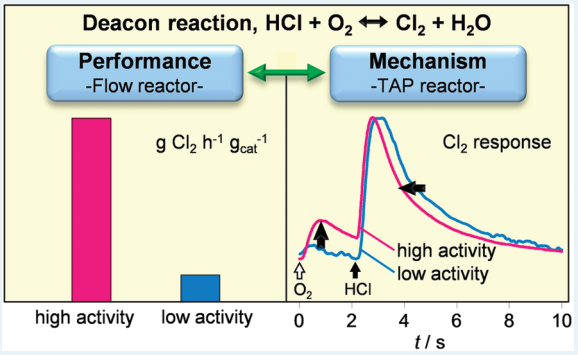

KEYWORDS: Deacon process, HCl oxidation, chlorine, Cr_2O_3, CeO_2, MnO_2, RuO_2, CuO, mechanism, temporal analysis of products

1. INTRODUCTION

Chlorine (Cl_2) is a major building block for the manufacture of important industrial chemicals and consumer products, such as plastics, solvents, textiles, agrochemicals and pharmaceuticals, insecticides, dyestuffs, cleaning products, etc. About one-half of the Cl_2 produced worldwide (>50 Mton per year) is reduced by its use to HCl or chloride salts.[1] For example, in the manufacture of polyurethanes, all of the chlorine used ends up as hydrogen chloride. The heterogenously catalyzed gas-phase oxidation of HCl to Cl_2 is an energy-efficient and environmentally sound way to recycle chlorine from HCl-containing industrial waste streams. However, in the past, researchers have encountered hurdles in identifying sufficiently active and stable catalysts for this reaction.

The catalytic route for chlorine production was first commercialized by Henry Deacon around 1870 using $CuCl_2$/pumice in a fixed-bed reactor at 693−723 K.[2] Deacon primarily conceived this process to curtail HCl emissions from the Leblanc process (production of soda ash). The resulting Cl_2 was then used to manufacture commercially valuable bleaching powder. Around 1900, the Solvay process "buried" the Leblanc process, and Cl_2 production was taken over by electrolysis. Renewed interest in HCl oxidation led Shell to establish in the 1960s a process using a $CuCl_2$−KCl/SiO_2 catalyst in a fluidized-bed reactor operated at 638 K.[3] The Shell process was apparently realized in a 30 kton Cl_2 per year facility,[4] but operation was eventually shut down.

Copper-based catalysts are not used in practice because of limited HCl conversion, fast catalyst deactivation due to volatilization of the active metal in the form of chlorides, and severe corrosion issues in the plant caused by unreacted HCl and product H_2O. Some of these disadvantages could be improved by conducting the chlorination (453−473 K) and the oxidation (613−673 K) steps over copper in two interconnected fluidized-bed reactors.[5] However, this configuration was not demonstrated on a large scale. In the 1980s, Mitsui introduced a process (MT-Chlor) using Cr_2O_3/SiO_2 in a fluidized-bed reactor operated at 623−703 K[6] and erected a plant that produces 60 kton of Cl_2 per year.[4]

A breakthrough in Cl_2 production via HCl oxidation has been achieved with the application of RuO_2-based materials: RuO_2/TiO_2-rutile (by Sumitomo, installed in a multitubular fixed-bed reactor at 473−653 K[4,7]) and RuO_2/SnO_2-cassiterite (by Bayer, installed in an adiabatic reactor cascade at 453−773 K[8,9]). Unlike copper and chromium-based catalysts, ruthenium-based catalysts

Received: February 12, 2011
Revised: March 20, 2011
Published: April 14, 2011

exhibit low-temperature activity and long lifetime. Detailed studies of RuO_2-based specimens (single crystals, polycrystalline powders, and supported systems) by means of state-of-the-art experimental and computational methods helped understanding the origin of their outstanding performance.[10−15] In essence, the self-regulating surface chlorination of RuO_2 and the choice of a support with rutile-type structure (TiO_2, SnO_2) to favor pseudomorphic growth are thought to be the key features for the catalyst stability. Furthermore, it has been shown that γ-Al_2O_3 added as binder to make RuO_2/SnO_2-cassiterite pellets acts as stabilizer, minimizing the interparticle sintering of the active Ru phase, thus perpetuating stable Cl_2 production over 7000 h.[9] Similarly, Sumitomo included SiO_2 in the formulation of the RuO_2/TiO_2-rutile catalyst to minimize RuO_2 sintering.[4]

Other than recent work on RuO_2, fundamental studies on the mechanism of the Deacon reaction over a wide range of oxide catalysts are scarce. The noxious and corrosive character of the reaction and the instability of many catalytic materials, often leading to metal volatilization above 700 K, may explain this lack. Thermochemical aspects of HCl oxidation were computed by Hisham and Benson[16] on a large set of metal oxides. Experiments entailing chlorination followed by oxidation (not relevant for accurate assessment of the catalytic performance) were also carried out on a set of oxides: namely, CuO, MnO_2, NiO, CoO, V_2O_5, MoO_3, Al_2O_3, and MgO. The process was analyzed on the basis of its dual-step nature, involving HCl absorption (chlorination) and Cl_2 production (reoxidation). Chlorination was found to be exothermic, fast, and accompanied by H_2O formation, whereas reoxidation was endothermic, very slow (except for CuO), and accompanied by Cl_2 evolution. The thermochemical properties derived in this study were not quantitatively correlated with the catalytic performance of the corresponding oxides, and the solids after reaction were not characterized in terms of phase and composition. In addition, catalysts of practical relevance, such as RuO_2 and Cr_2O_3, or less studied catalytic systems, such as CeO_2, were not assessed. Thus, a deeper mechanistic understanding of the catalyzed HCl oxidation is required. The attainment of mechanistic descriptors of Deacon catalysts, being able to account for their activity and selectivity, is advantageous for developing new suitable formulations as well as for optimizing existing systems.

Transient (dynamic, unsteady-state) methods can be advantageously used to study mechanisms of industrially relevant and experimentally demanding reactions over heterogeneous catalysts.[17,18] Among those, the temporal analysis of products (TAP) technique[19−21] holds a prominent role, namely due to (i) the millisecond time resolution, (ii) the use of practical catalysts, (iii) the excellent temperature control, and (iv) the safe operation. We have recently proven that TAP is a powerful technique to study mechanistic aspects of the Deacon reaction over ruthenium- and copper-based catalysts.[15,22]

Herein, we have extended TAP investigations on HCl oxidation, complemented by catalytic testing in a flow reactor at ambient pressure, to other relevant catalysts: Cr_2O_3 (applied in the MT-Chlor process[6]), MnO_2 (used by Scheele in the first experiment to produce Cl_2 back in 1774), and (iii) CeO_2 (whose Deacon activity has been noticed[23]). These three oxides plus the previously studied RuO_2 and CuO conform a representive set of

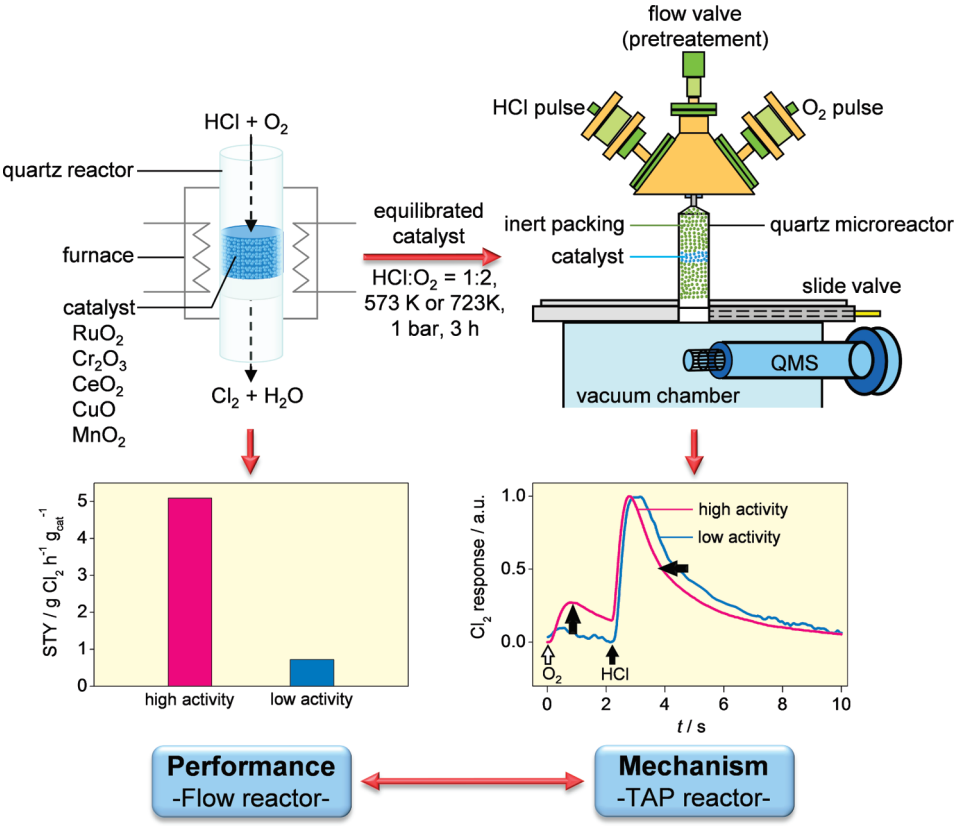

Figure 1. The catalytic performance of metal oxides in HCl oxidation has been assessed in a continuous-flow reactor at ambient pressure (left) and correlated with mechanistic features, gathered by measurements in the TAP reactor (right). The latter were carried out on flow-equilibrated samples to ensure that no alteration of the state of the catalyst would take place along the mechanistic investigations.

dx.doi.org/10.1021/cs200075j |ACS Catal. 2011, 1, 583–590

samples to derive correlations between mechanistic footprints and catalytic performance. Because the state of the catalysts changes more or less extensively or rapidly (or both) upon contact with the reaction mixture until a steady-state composition is reached,[12,22] TAP studies were carried out on flow-equilibrated catalysts to secure that the mechanism would be assessed over stable samples (Figure 1).

2. EXPERIMENTAL SECTION

2.1. Catalysts and Characterization. CeO_2 (Aldrich, nanopowder) and Cr_2O_3 (Aldrich, nanopowder, 99%) were heated in static air at 773 K (10 K min^{-1}) for 5 h prior to their use, and MnO_2 (Strem, 99.995%) was used as received. RuO_2 and CuO were employed as reference materials. RuO_2 (Aldrich, 99.9%) underwent the same pretreatment as CeO_2 and Cr_2O_3, while CuO was obtained by heating of $Cu(NO_3)_2 \cdot 3H_2O$ (Alfa Aesar, 98%) in static air at 873 K (5 K min^{-1}) for 15 h. The samples (before and after the catalytic tests described in Section 2.2) were characterized by X-ray diffraction and N_2 adsorption. Powder X-ray diffraction (XRD) was measured in a PANanalytical X'Pert PRO-MPD diffractometer. Data were recorded in the range 10−70° 2θ with a step size of 0.017° and a counting time of 0.26 s/step. Nitrogen adsorption at 77 K was measured in a Quantachrome Quadrasorb-SI gas adsorption analyzer. Prior to the measurement, the samples were degassed in vacuum at 473 K for 10 h.

2.2. Catalytic Tests. The oxidation of HCl with O_2 was studied at 723 K in a quartz fixed-bed microreactor (8 mm i.d.) using 0.5 g of catalyst (particle size = 0.4−0.6 mm), a total flow of 166 cm^3 STP min^{-1}, and atmospheric pressure. Due to its high intrinsic catalytic activity,[22] RuO_2 was tested at 573 K using 0.25 g of sample. The feed mixture (hereafter denoted as the Deacon mixture) contained 10 vol % HCl (Messer, purity 2.8, anhydrous) and 20 vol % O_2 (Pan Gas, purity 5.0), balanced in N_2 (Pan Gas, purity 5.0). The samples were heated in N_2 to the reaction temperature, followed by the introduction of the Deacon mixture over 3 h. Quantitative Cl_2 analysis during the isothermal tests was done at sampling periods of 60 min by iodimetric titration in a Mettler Toledo G20 compact titrator using the protocol reported elsewhere.[22]

2.3. Temporal Analysis of Products. Transient mechanistic studies were carried out in the TAP-2 reactor[19,20] over equilibrated CeO_2, Cr_2O_3, and MnO_2 samples, as illustrated in Figure 1. The term "equilibrated" is extensively used throughout this article and refers to the fact that the samples were previously exposed to the Deacon mixture according to the procedure described in Section 2.2. The advantage of this protocol is that the 3-h catalytic test at ambient pressure sets the samples in a stabilized form, which will not be altered during the TAP experiments due to the very small amount of reactants pulsed (see below). This makes it possible to conduct "state-defining" experiments,[19] in which mechanistic information is obtained without perturbing the state of the catalyst. Alteration of the catalyst in the course of the reaction is a serious limitation of many mechanistic/kinetic techniques, and this is particularly relevant here, given the dynamic nature of the catalysts during HCl oxidation.

The samples (20 mg, particle size = 0.2−0.3 mm) were loaded in the isothermal (central) zone of a quartz microreactor (4.6 mm i.d.), between two layers of quartz particles of the same particle size. The thickness of the catalyst zone (2−2.5 mm) was very small compared with the overall bed length (71 mm). This configuration, referred to as thin-zone reactor, is characterized by negligible gas concentration gradients across the catalyst bed.[24] The samples were pretreated in 20 cm^3 STP min^{-1} of He at 623 K and 1 bar for 1 h, followed by evacuation the reactor to 10^{-10} bar. The following pulse experiments were carried out in high vacuum at 623 K for RuO_2 and at 723 K for all other catalysts, using a pulse size of 10^{16} molecules:

(a) Simultaneous pulsing of O_2/Ar = 2:1 and HCl/Kr = 5:1.
(b) Pump−probe experiments of O_2/Ar = 2:1 and HCl/Kr = 5:1, also referred to as sequential pulsing. In these experiments, the O_2/Ar mixture was pulsed first and then the HCl/Kr mixture, separated by a time delay (Δt) ranging from 1 to 4 s. The pump and probe pulses were repeated cyclically, keeping constant in all cases a time interval of 10 s between the probe pulse of one cycle (HCl/Kr) and the pump pulse of the following cycle (O_2/Ar).

In the TAP experiments, Kr (Linde, purity 5.0), Ar (Linde, purity 5.0), Cl_2 (Linde, purity 4.0), O_2 (Air Products, purity 5.2), and HCl (Praxair, purity 2.5) were used. A quadrupole mass spectrometer (RGA 300, Stanford Research Systems) monitored the transient responses at the reactor outlet of the following atomic mass units (AMUs): 84 (Kr), 70 (Cl_2), 40 (Ar), 36 (HCl), 32 (O_2), and 18 (H_2O). The responses displayed in this paper correspond to an average of 10 pulses per AMU to improve the signal-to-noise ratio. Prior to that, it was checked that the responses were stable; that is, with invariable intensity and shape during at least 20 consecutive pulses.

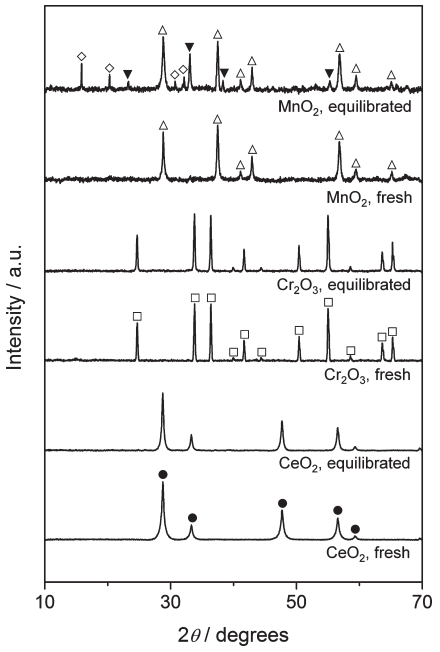

Figure 2. X-ray diffraction patterns of the starting oxides (fresh) and the samples after ambient-pressure Deacon tests (equilibrated). Phases: (●) CeO_2, JCPDS 04-0593, (□) Cr_2O_3, JCPDS 70-3766, (△) MnO_2, JCPDS 81-2261, (▼) Mn_2O_3, JCPDS 71-3820, and (◊) $MnCl_2 \cdot 2H_2O$, JCPDS 25-1043.

3. RESULTS AND DISCUSSION

3.1. Catalytic Activity at Ambient Pressure. The oxidation of HCl over Cr_2O_3, CeO_2, MnO_2, CuO, and RuO_2 was studied in a continuous-flow reactor at a total pressure of 1 bar and at 723 K

dx.doi.org/10.1021/cs200075j |ACS Catal. 2011, 1, 583–590

Table 1. STY of Cl_2 for the Catalysts in Deacon Tests under Flow Conditions and Characteristic Times (t^*_{max} and $t_{h/5}$) of the Cl_2 and H_2O Responses in the TAP Reactor upon Simultaneous Pulsing of O_2 and HCl

		Cl_2		H_2O	
sample	STY[a] (g Cl_2 h^{-1} g_{cat}^{-1})	t^*_{max}[b] (s)	$t_{h/5}$[b] (s)	t^*_{max} (s)	$t_{h/5}$ (s)
Cr_2O_3	1.15	0.24	1.56	0.28	2.40
CeO_2	0.77	0.21	3.85	0.31	2.39
MnO_2	0.03	0.38	3.35	0.06	0.96
RuO_2[c]	5.09	0.20	2.00	0.25	3.19
CuO[c]	0.72	0.31	2.32	0.002	0.84

[a] After 3 h in the Deacon mixture; experimental conditions in Section 2.2. [b] Time of maximum (t^*_{max}) and width at 1/5 of the height ($t_{h/5}$) of the normalized transient responses, determined as shown in Figure 5. [c] Transient responses of these samples were reported in ref 22.

(573 K for RuO_2). The catalysts were constituted by pure phase oxides. In fact, the X-ray diffraction patterns of the fresh samples (Figure 2 and ref 22) exclusively exhibited the characteristic reflections of chromium(III) oxide, cerium(IV) oxide, manganese(IV) oxide, copper(II) oxide, and ruthenium(IV) oxide. The total surface area (S_{BET}) of the fresh oxides is 106, 10, and 1 m^2 g^{-1} for CeO_2, Cr_2O_3, and MnO_2, respectively. The latter two values resemble those determined for RuO_2 and CuO (10 and 2 m^2 g^{-1}, in that order).[22] The Deacon activity of the metal oxides remained essentially constant in the course of the 3-h test. The activity, expressed in terms of space time yield (STY, grams of Cl_2 per hour per gram of catalyst), is reported in Table 1.

Comparing these results, the following activity order is derived: RuO_2 > Cr_2O_3 > CeO_2 ~ CuO > MnO_2. The performance of RuO_2 remains unrivalled, despite the testing's being carried out at a significantly lower temperature and with the half of the catalyst amount. The low temperature activity of RuO_2 indeed constituted one of the major reason for the success of this metal oxide, determining its industrial development and implementation for large scale Cl_2 production.[4,8,9] Cr_2O_3 is ~5 times less active than RuO_2. The STY of CeO_2 and CuO are similar and a third lower with respect to Cr_2O_3. MnO_2 exhibits the lowest activity. This latter outcome is expected because the Cl_2 liberation step was reported to be favored only at temperatures above ~833 K.[16]

The catalysts equilibrated in HCl oxidation were investigated to assess eventual modifications of their textural properties, chemical composition, and structure. The S_{BET} showed no significant changes in the case of Cr_2O_3 and MnO_2 (9 and 1 m^2 g^{-1}, respectively), whereas the S_{BET} of CeO_2 decreased to 27 m^2 g^{-1} upon use, suggesting a rather relevant degree of sintering of the CeO_2 crystallites. Some degree of particle agglomeration upon HCl oxidation was also reported for RuO_2.[10] Structure-wise, the diffractograms of equilibrated CeO_2 and Cr_2O_3 (Figure 2) did not reveal any detectable phase variation, indicating that the bulk structure of these catalysts was not altered upon exposure to reaction conditions and, therefore, that chlorination is limited to the surface or near-surface; that is, only a few layers deep. In this respect, these systems resemble RuO_2, for which self-regulating surface chlorination was evidenced.[10,12]

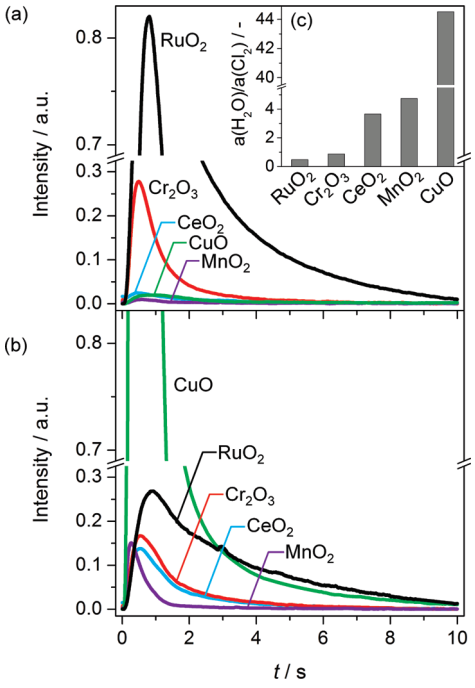

Figure 3. Transient responses of (a) Cl_2 and (b) H_2O upon simultaneous pulsing of O_2 and HCl over equilibrated CeO_2, Cr_2O_3, and MnO_2. The inset (c) shows the ratio of areas of reaction products.

In contrast, Mn_2O_3 and $MnCl_2 \cdot 2H_2O$ were detected in appreciable amounts in the XRD pattern of equilibrated MnO_2, in addition to the still dominant MnO_2 phase, indicating that bulk alteration of the starting oxide is considerable. This behavior compares with that of CuO because $CuCl_2 \cdot 2H_2O$ and CuCl appeared as prevalent phases, along with some residual CuO and Cu(OH)Cl, in the used sample,[22] although the bulk chlorination of MnO_2 looks less extensive. On the basis of this evidence, chlorination limited to the surface seems to correlate with a higher catalytic activity (RuO_2, Cr_2O_3, CeO_2), and bulk chlorination results either in fast deactivation due to volatilization of the active phase (CuO) or in very low activity (MnO_2).

3.2. Temporal Analysis of Products. TAP experiments comprised simultaneous and sequential (pump−probe) pulsing of O_2 and HCl over the equilibrated oxides. The total amount of HCl dosed per sample was in the order of 0.004 mmol, contrasting with the 0.134 mmol of HCl to which each sample was exposed in the ambient-pressure catalytic tests. Consequently, the X-ray diffraction patterns of the samples after TAP experiments experienced no change (diffractograms not shown, see Figure 2, equilibrated samples). This result corroborates our previous reasoning on the importance of equilibration in order to determine mechanistic features on stabilized samples.

Simultaneous pulsing of O_2 and HCl. Figure 3 depicts the transient responses of products upon simultaneous pulsing of O_2 and HCl over Cr_2O_3, CeO_2, and MnO_2 at 723 K. The responses obtained over RuO_2 and CuO are reproduced from our previous study.[22] Both reaction products were clearly detected, validating the use of the TAP reactor to study the Deacon reaction on this new set of materials. Comparing the intensities of the Cl_2 responses, the following activity order can be derived: RuO_2 > Cr_2O_3 > CeO_2 ~ CuO > MnO_2. This sequence is in qualitative

dx.doi.org/10.1021/cs200075j |ACS Catal. 2011, 1, 583–590

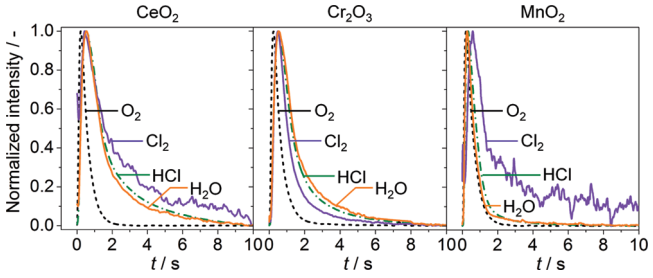

Figure 4. Normalized transient responses of reactants and products upon simultaneous pulsing of O_2 and HCl over equilibrated CeO_2, Cr_2O_3, and MnO_2.

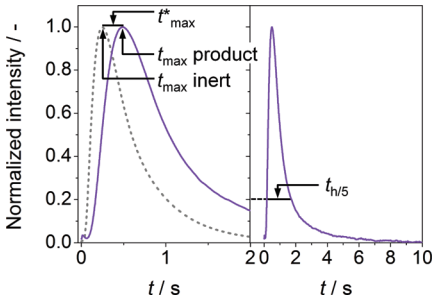

Figure 5. Determination of characteristic times (t^*_{max} and $t_{h/5}$) from the transient responses of Cl_2 and H_2O. The corresponding values for the various oxides are collected in Table 1.

agreement with the results of the steady-state experiments at 1 bar (Table 1), despite the low-pressure and dynamic operation in the TAP reactor.

By analysis of the ratio of the areas of their responses (Figure 3c), interesting mechanistic insights can be derived from the relative amounts of H_2O and Cl_2 formed. The ratio surpassed 1 for CuO, CeO_2, and MnO_2, indicating that H_2O formation is much easier than Cl_2 formation. Conversely, the H_2O/Cl_2 ratio resulted in slightly less than 1 for Cr_2O_3 and about 0.5 for RuO_2. In the case of CuO, the extremely high relative water production was explained on the basis of the extensive interaction of HCl with bulk oxygen species and the easy hydroxyl recombination from the copper hydroxychloride species generated, whereas the low Cl_2 production was traced back to the high stability of the copper chlorides formed upon H_2O release.[22] When considering the case of MnO_2, the remarkable bulk changes observed upon equilibration, though more limited than for CuO, suggest that the reasons described for the more favorable H_2O production on CuO likely hold for MnO_2, as well. In the case of CeO_2, XRD analysis revealed no bulk chlorination upon use, as for RuO_2 and Cr_2O_3. The origin of the opposite behavior of these latter oxides in terms of relative production of H_2O and Cl_2 will be further tackled on the basis of mechanistic parameters herein introduced.

Figure 4 represents the normalized transient responses of reactants and products upon simultaneous pulsing of O_2 and HCl over Cr_2O_3, CeO_2, and MnO_2 at 723 K. Normalization of the profiles enables distinguishing of the production and adsorption/desorption kinetics of the reaction products. The normalized responses were characterized by two parameters: namely, the time of maximum (t^*_{max}) and the width at 1/5 of the height ($t_{h/5}$). t^*_{max} is defined as the time of maximum of the product subtracted by the time of maximum of the inert gas (always pulsed with the reactive gas, see the Experimental section). The correction by the inert gas is intended to remove the effect of small time shifts that might arise between the different reactor loads and operation of the high-speed pulse valves, leading to a more reliable comparison of the various oxides. Up to this point, t^*_{max}, the flow is described by a convective regime because the initial pulse size of 10^{16} molecules exceeds the Knudsen regime (above 5×10^{14} molecules). Under these conditions, the product gases are swept from the catalyst zone by the inert and reactant gas flows, and readsorption of products is negligible. Therefore, t^*_{max} provides good assessment of the initial production rate.

The other characteristic time, $t_{h/5}$, corresponds to the time needed for elution of 80% of the product formed. This point is located in the decay region of the responses. Because the pressure in the reactor is at this point lower than that required for convective flow, the Knudsen regime dominates. The shape of the decay curve is then determined by the surface lifetime of the products. Thus, the more quickly this point is reached, the shorter the surface lifetime (i.e., shorter $t_{h/5}$) and vice versa. Accordingly, $t_{h/5}$ offers an estimation of the adsorption/desorption kinetics and seems to be a better parameter than the formerly used $t_{h/2}$.[22] Eventual tailings of the responses, indicative of difficult product desorption or favored readsorption (or both), become, in fact, more pronounced at longer times. Therefore, differences in behavior become more distinguishable, particularly in the comparison of transients of products obtained from various catalysts (see Figure 4). The smaller the values of these parameters are, the faster the production/desorption is. Figure 5 offers a graphical illustration of these parameters, and their corresponding values for the oxides are listed in Table 1.

The characteristic parameters were in the first instance correlated with the activity observed in the isothermal experiments at ambient pressure for the metal oxides, aiming at discriminating their different performances in Cl_2 production on the basis of mechanistic features. Qualitative trends for the STY versus t^*_{max} and $t_{h/5}$ of Cl_2 were derived from Table 1. The first approach was based on the correlation of the individual TAP-derived parameters with the STY (not shown). Accordingly, the most active catalyst (highest STY), RuO_2, had the lowest t^*_{max} for Cl_2 among all oxides, but a longer $t_{h/5}$ for Cl_2 with respect to Cr_2O_3. Such a conflicting situation was also observed when comparing Cr_2O_3 and CeO_2, the t^*_{max} for Cl_2 of Cr_2O_3 being higher than that of CeO_2, even though the former material was more active. Because the individual parameters contain different but complementary physicochemical information, we concluded that both should be taken into account to explain the activity order. Thus, combinations of t^*_{max} and $t_{h/5}$ of Cl_2 were considered.

The best descriptor for the ambient-pressure activity yielded the product of the characteristic transient parameters ($t^*_{max} \times t_{h/5}$), as depicted in Figure 6a. Accordingly, the catalyst with the shortest t^*_{max} and $t_{h/5}$ of Cl_2 corresponds to the most active system; that is, a highly active catalyst should, in fact, enable both a fast production and desorption of Cl_2 and should not suffer from product inhibition.

RuO_2, with the largest STY, has the smallest value of the product of t^*_{max} and $t_{h/5}$, whereas MnO_2, with the smallest STY, gives the largest value. Because the isothermal test over RuO_2 was carried out at a lower temperature (573 K) than the other metal oxides, the very fast Cl_2 production, coupled with a relatively fast

dx.doi.org/10.1021/cs200075j |ACS Catal. 2011, 1, 583–590

desorption, explain very well the outstanding activity of RuO_2. Although Cl_2 production is a bit delayed for Cr_2O_3, desorption of Cl_2 has the most favorable kinetics, making this catalyst the second-most-active oxide among the others of this study.

For CeO_2, the production of Cl_2 is very fast (shortest t^*_{max}); however, its activity is controlled by Cl_2 desorption, which is highly impeded (very long $t_{h/5}$). Alternatively, readsorption of Cl_2 might be a favored process, that is, product inhibition. In any case, the value of the product of t^*_{max} and $t_{h/5}$ shifts to the right, and this catalyst shows as less active than Cr_2O_3.

CuO, with activity close to that of CeO_2, shows a more impeded Cl_2 production (long t^*_{max}) with respect to CeO_2. The similar activity of CeO_2 and CuO can be explained by the shorter $t_{h/5}$ of Cl_2 for CuO. In fact, the effects of t^*_{max} and $t_{h/5}$ of Cl_2 on the product compensate each other. The low activity of MnO_2 is related to the very long t^*_{max} (very difficult Cl_2 formation) coupled with a very long $t_{h/5}$ (extremely difficult desorption or significant readsoption), in agreement with the literature.[16]

Analysis of the transients by means of t^*_{max} and $t_{h/5}$ leads to clear insights into the origin of the higher amount of H_2O produced by CuO, CeO_2, and MnO_2 with respect to Cl_2 (Figure 3). The $t_{h/5}$ values for H_2O are lower than for Cl_2, accounting for a faster H_2O evolution. For CuO and MnO_2, even the t^*_{max} of H_2O is significantly smaller than that of Cl_2. Thus, both production (t^*_{max}) and desorption ($t_{h/5}$) are faster in the case of H_2O with respect to Cl_2.

Further, a trend for the dependence of the space time yield in flow experiments on the ratio of $t_{h/5}$ of Cl_2 and $t_{h/5}$ of H_2O (i.e. relative desorption of products) was obtained (Figure 6b). The higher this ratio, the lower the activity of the catalyst. Consistently, the ratio for RuO_2 falls in the range of lower values, whereas for MnO_2, it is in the higher value range. Cr_2O_3, CeO_2, and CuO, with moderate activities, are located in the middle zone. This behavior is tentatively attributed to the fact that the catalysts that desorb Cl_2 faster (low $t_{h/5}$ Cl_2) than H_2O free more active sites for the reaction to proceed. On the basis of a mechanism recently illustrated for RuO_2, Cl_2 desorption, in fact, generates two active sites, whereas H_2O desorption creates only one active site.[10]

Pump−Probe Experiments. Pump−probe experiments between O_2 and HCl were carried out at 723 K over CeO_2, Cr_2O_3, and MnO_2 and at 623 K over RuO_2. The time delay between the pump and probe pulse (Δt) was varied in the 1−4 s range. The consecutive cycles were linked in such a way that the time elapsed between the probe and the pump pulse in the next cycle was always equal to 10 s. After this time, the probe pulse has almost eluted, and the coverage of the probe molecule at the beginning of the cycle is, therefore, very low.

Pump−probe experiments enable the features related to the two steps of HCl oxidation—catalyst chlorination (HCl pulsing) and catalyst reoxidation (O_2 pulsing)—to be evaluated separately. The transient responses of Cl_2 obtained in these experiments are presented in Figure 7. The profiles are characterized by Cl_2 production on HCl pulsing, common to all oxides, and by Cl_2 production on O_2 pulsing, only detected in the case of RuO_2 and CeO_2. Considering the former component for MnO_2, Cr_2O_3, and CeO_2, it is at first glance clear that the intensities of the Cl_2 responses are independent of the time delay (Δt) between O_2 and HCl pulsing. Sustained Cl_2 production, even at low oxygen

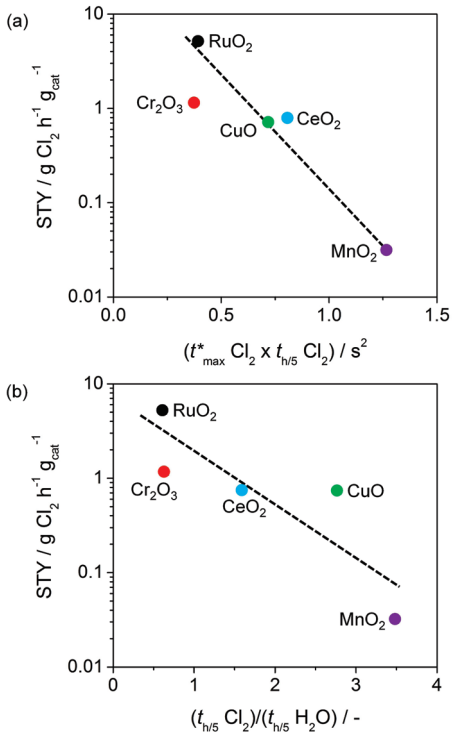

Figure 6. Correlation between the space time yield for the catalysts resulting from ambient-pressure Deacon tests and characteristic parameters derived from the Cl_2 and H_2O responses in the TAP reactor on simultaneous pulsing of O_2 and HCl.

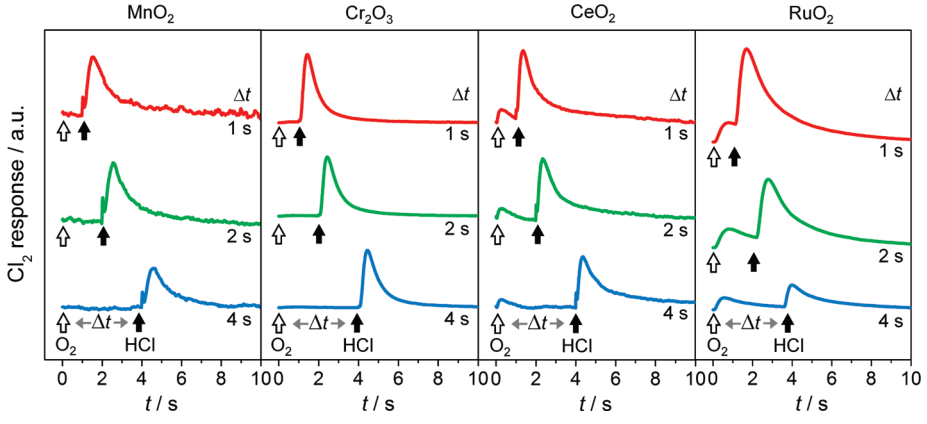

Figure 7. Transient Cl_2 responses in pump−probe experiments with O_2 and HCl at variable time delay (Δt) over the equilibrated catalysts.

dx.doi.org/10.1021/cs200075j |ACS Catal. 2011, 1, 583–590

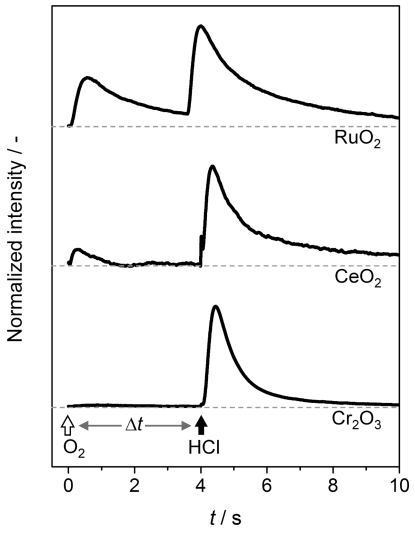

Figure 8. Normalized transient Cl_2 responses in pump−probe experiments with O_2 and HCl (Δt = 4 s) over the equilibrated catalysts.

surface coverage (i.e., at high Δt values), indicates that lattice oxygen species take part in the reaction.

Qualitatively similar results were, in fact, obtained for CuO.[22] Still, on the basis of XRD analysis, the extent of lattice involvement must be different for the three oxides here examined. Due to the significant bulk changes experienced by MnO_2, participation of bulk oxygen species (i.e. chlorine production independent of the oxygen surface coverage) was expected for this oxide. On the other hand, no bulk compositional modifications, at least by powder X-ray diffraction, were observed for Cr_2O_3 and CeO_2 (Figure 2). Because these pump−probe experiments strongly suggest involvement of lattice oxygen, it is deduced that active lattice species in these two oxides should be only those at the surface level or in a few subsurface layers, and bulk atoms do not participate in HCl oxidation. Surface chlorination was reported for RuO_2, as well.[12] However, for RuO_2, a progressive decrease in intensity of the Cl_2 response on increasing the time delay of HCl pulsing is revealed (Figure 7), indicating that the Cl_2 production strongly depends on the oxygen coverage and that the reaction basically obeys a Langmuir−Hinshelwood mechanism.[15]

Let us finally discuss the Cl_2 release upon reoxidation (O_2 pulsing). As mentioned, this feature is observed only in the case of RuO_2 and CeO_2, the former producing more chlorine than the latter. Analysis of their normalized transients (Figure 8), compared with the other most active oxide, Cr_2O_3, leaves open the possibility that Cl_2 produced upon HCl pulsing might not be fully evolved from the two systems, even after 10 s, although Cl_2 production upon O_2 pulsing should not be interpreted as further release of the residual chlorine, but rather, as a consequence of the intrinsic reoxidation capability of the material (i.e. oxygen-assisted chlorine removal), as recently shown for $RuO_{2-x}Cl_x$-(110).[25] In fact, (i) release of residual chlorine would not appear with a pulse shape, and (ii) also in the case of Cr_2O_3, the surface is still chlorinated, but no chlorine is liberated. The absence/presence and, in turn, intensity of this signal thus constitute a clear indication of the ease of reoxidation of the oxide. Accordingly, reoxidation of RuO_2 is favorable, quite favorable for CeO_2, more hindered for Cr_2O_3, and impeded for MnO_2 and CuO. The fact that Cr_2O_3 is more active than CeO_2, albeit reoxidation is more favorable for the latter, traces back to the easier Cl_2 desorption; that is, less broad Cl_2 response at HCl pulsing, in agreement with the discussion of the results of the simultaneous pulsing of O_2 and HCl previously proposed.

4. CONCLUSIONS

In this study, we have successfully correlated the catalytic performance in Cl_2 production by HCl oxidation of a representative set of metal oxides with mechanistic descriptors derived from temporal analysis of products studies. Although XRD phase analysis of fresh and equilibrated samples provides a basic discrimination of the catalysts' performance on the basis of the involvement/exclusion of bulk lattice species in the reaction (bulk chlorination), the characteristic transient parameters here introduced allow a deeper relation of the ambient-pressure activity to key steps of the reaction mechanism, such as chlorine recombination and desorption as well as catalyst reoxidation. The ranking of the catalysts in terms of Deacon activity appeared as $RuO_2 > Cr_2O_3 > CeO_2 \sim CuO > MnO_2$. The least performing catalysts, MnO_2 and CuO, showed bulk chlorination, highly impeded Cl_2 evolution, and difficult reoxidation. For the oxides with moderated activity, Cr_2O_3 and CeO_2, participation of lattice species was limited to the (near-)surface, but the overall activity was limited by a less favored reoxidation or Cl_2 desorption. The most active oxide, RuO_2, combines the three crucial features for an optimal catalyst: limited surface chlorination to favor long-term stability; fast Cl_2 evolution; and relatively easy reoxidation, thus allowing low-temperature operation.

AUTHOR INFORMATION

Corresponding Author

*Fax: +41 44 633 1405. E-mail: jpr@chem.ethz.ch.

ACKNOWLEDGMENT

Bayer MaterialScience AG is acknowledged for permission to publish these results. Discussions with Dr. Timm Schmidt were highly appreciated. We thank reviewer no. 2 for insightful comments on the interpretation of the characteristic time parameters in the transient responses.

REFERENCES

(1) Motupally, S.; Mah, D. T.; Freire, F. J.; Weidner, J. W. *Electrochem. Soc. Interface* **1998**, *7*, 32–36.
(2) Deacon, H. U.S. patent 85,370, 1868.
(3) Engel, W. F.; Wattimena, F. U.S. patent 3,210,158, 1965.
(4) Seki, K. *Catal. Surv. Asia* **2010**, *14*, 168–175.
(5) Mortensen, M.; Minet, R. G.; Tsotsis, T. T.; Benson, S. *Chem. Eng. Sci.* **1999**, *54*, 2131–2139.
(6) Kiyoura, T.; Kogure, Y.; Nagayama, T.; Kanaya, K. U.S. patent 4,822,589, 1989.
(7) Abekawa, H.; Ito, Y.; Hibi, T. U.S. patent 5,908,607, 1999.
(8) Wolf, A.; Mleczko, L.; Schluter, O. F.; Schubert, S. U.S. patent US 2007/0274897.
(9) Mondelli, C.; Amrute, A. P.; Krumeich, F.; Schmidt, T.; Pérez-Ramírez, J. *ChemCatChem* **2011**, *3*, 657−660.
(10) López, N.; Gómez-Segura, J.; Marín, R. P.; Pérez-Ramírez, J. *J. Catal.* **2008**, *255*, 29–39.
(11) Zweidinger, S.; Crihan, D.; Knapp, M.; Hofmann, J. P.; Seitsonen, A. P.; Weststrate, C. J.; Lundgren, E.; Andersen, J. N.; Over, H. *J. Phys. Chem. C* **2008**, *112*, 9966–9969.

(12) Crihan, D.; Knapp, M.; Zweidinger, S.; Lundgren, E.; Weststrate, C. J.; Andersen, J. N.; Seitsonen, A. P.; Over, H. *Angew. Chem., Int. Ed.* **2008**, *47*, 2131–2134.
(13) Zweidinger, S.; Hofmann, J. P.; Balmes, O.; Lundgren, E.; Over, H. *J. Catal.* **2010**, *272*, 169–175.
(14) Studt, F.; Abild-Pedersen, F.; Hansen, H. A.; Man, I. C.; Rossmeisl, J.; Bligaard, T. *ChemCatChem* **2010**, *2*, 98–102.
(15) Hevia, M. A. G.; Amrute, A. P.; Schmidt, T.; Pérez-Ramírez, J. *J. Catal.* **2010**, *276*, 141–151.
(16) Hisham, M. W. M.; Benson, S. W. *J. Phys. Chem.* **1995**, *99*, 6194–6198.
(17) Berger, R. J.; Kapteijn, F.; Moulijn, J. A.; Marin, G. B.; Wilde, J. D.; Olea, M.; Chen, D.; Holmen, A.; Lietti, L.; Tronconi, E.; Schuurman, Y. *Appl. Catal., A* **2008**, *342*, 3–28.
(18) Kondratenko, E. V. *Catal. Today* **2010**, *157*, 16–23.
(19) Gleaves, J. T.; Yablonsky, G. S.; Phanawadee, P.; Schuurman, Y. *Appl. Catal., A* **1997**, *160*, 55–88.
(20) Pérez-Ramírez, J.; Kondratenko, E. V. *Catal. Today* **2007**, *121*, 160–169.
(21) Gleaves, J. T.; Yablonsky, G.; Zheng, X.; Fushimi, R.; Mills, P. L. *J. Mol. Catal. A: Chem.* **2010**, *315*, 108–134.
(22) Amrute, A. P.; Mondelli, C.; Hevia, M. A. G.; Pérez-Ramírez, J. *J. Phys. Chem. C.* **2011**, *115*, 1056–1063.
(23) Lee, G.; Lee, S. W.; Sohn, I.; Kwon, Y. C.; Song J.; Son, C.-S. WO 2009/035234.
(24) Shekhtman, S. O.; Yablonsky, G. S.; Chen, S.; Gleaves, J. T. *Chem. Eng. Sci.* **1999**, *54*, 4371–4378.
(25) Hofmann, J. P.; Zweidinger, S.; Seitsonen, A. P.; Farkas, A.; Knapp, M.; Balmes, O.; Lundgren, E.; Andersen, J. N.; Over, H. *Phys. Chem. Chem. Phys.* **2010**, *12*, 15358–15366.